Pergamon

SCIENCE DIRECT®

Bioorganic & Medicinal Chemistry 11 (2003) 1643–1652

BIOORGANIC & MEDICINAL CHEMISTRY

Synthesis, Cellular Internalization and Photodynamic Activity of Glucoconjugated Derivatives of Tri and Tetra(*meta*-hydroxyphenyl)chlorins

I. Laville,[a] T. Figueiredo,[b] B. Loock,[b] S. Pigaglio,[a] Ph. Maillard,[b] D. S. Grierson,[b] D. Carrez,[c] A. Croisy[c] and J. Blais[a,*]

[a]*LPBC, UMR CNRS 7033 and Université Pierre et Marie Curie, 4 Place Jussieu, case 138, 75252 Paris Cedex 05, France*
[b]*UMR 176 CNRS-Institut Curie, Section de Recherche, Bat 110 Centre Universitaire, 91405 Orsay, France*
[c]*INSERM U-350, Institut Curie, Section de Recherche, Bat 112 Centre Universitaire, 91405 Orsay, France*

Received 18 October 2002; accepted 17 January 2003

Abstract—Glucoconjugated tri and tetra(*meta*-hydroxyphenyl)chlorins have been synthesized in order to explore how glucoconjugation of the macrocycle affects the photoactivity of the molecule. Internalization processes, photosensitizing efficacy of TPC(*m*-*O*-GluOH)$_3$ and TPC(*m*-*O*-GluOH)$_4$, in HT29 human adenocarcinoma cells have been compared to those of tetra(*meta*-hydroxyphenyl)chlorin (*m*-THPC, Foscan®). The tetra glucoconjugated chlorin, TPC(*m*-*O*-GluOH)$_4$, was found to be poorly internalized and weakly photoactive. In contrast, the asymmetric and more amphiphilic compound TPC(*m*-*O*-GluOH)$_3$, exhibited superior phototoxicity compared to *m*-THPC. Drug concentration, temperature and sodium azide effects indicated that TPC(*m*-*O*-GluOH)$_3$ internalization partly proceeds via an active receptor-mediated endocytosis mechanism. Cellular uptake appeared as a saturable process and remained 30% lower than for *m*THPC. However, a maximum phototoxicity in HT29 cells (survival fraction of $2\pm0.6\%$) were observed for concentration as low as 2 μM. A 4-fold higher concentration of *m*-THPC was necessary to observe the same level of photoactivity. This higher phototoxicity has been correlated to a greater mitochondrial affinity. On the basis of these results, work is in progress to further evaluate the potential of glycosylated chlorins in photodynamic therapy (PDT).

Introduction

Photodynamic therapy (PDT) is now well established as a clinical treatment modality for both neoplasic and non-neoplasic diseases.[1] In this context, a number of chlorin, phthalocyanine and benzoporphyrin based photosensitizers have been developed[2] which compared to Haematoporphyrin derivatives (HpD), and its commercial version Photofrin®, exhibit improved photodynamic activity. Among them, the tetra-(*meta*-hydroxyphenyl)-chlorin (*m*-THPC, Foscan®)[3,4] received regulatory approval in 2002 in the European Union for human palliative treatment of head and neck cancers.

Long-term cutaneous photosensitivity and necrosis of surrounding normal tissues upon exposure to light is often observed in antitumor photodynamic therapy due to a poor selectivity of the photosensitizer. Targeting of photosensitizing agents to tumor cells thus appears as a viable means to circumvent these problems, and to thereby achieve a higher efficacy for PDT treatment through the administration of lower doses to patients.

Several strategies have been proposed to improve the tumor selectivity of photosensitizers. These include the use of adapted delivery systems such as liposomes, lipoproteins, monoclonal antibodies, nanoparticles (for review see ref 5) to modify the drug biodistribution, and the use of long-circulating carriers to increase in vivo PDT efficacy of certain photosensitizers.[6–8]

Another approach developed by several groups is to modulate the amphiphilicity of the photosensitizer.[9] Indeed, a correlation has been established between the photoefficacy and the partition coefficient for both Zn phthalocyanines[10] and other porphyrin derivatives.[11] Structural modifications induced by glycoconjugation of the tetrapyrrole system appears as an effective means to create a balance between hydrophilicity and hydrophobicity. Moser et al.[12] observed a 50–100-fold higher phototoxicity for diglucoamido porphyrinoids compared

*Corresponding author. Tel.: +33-1-4427-7546; fax +33-1-4427-7560; e-mail: jblais@lpbc.jussieu.fr

0968-0896/03/$ - see front matter © 2003 Elsevier Science Ltd. All rights reserved.
doi:10.1016/S0968-0896(03)00050-6

to the non glucosylated analogues with various melanoma cell lines. An improvement in the phototoxicity of mono-glycosylated porphyrin derivatives relative to Photofrin against K562 leukaemia cells has also been reported.[13,14] Recently, Pandey and co-workers[15] established a quantitative structure–activity relationship for galactosylated chlorins, demonstrating that the presence and the position of the sugar substituent is crucial to photobiological activity. Following this approach, in the last decade, a series of neutral tri- and tetra-glycosylated porphyrins in which mono- or disaccharides are linked via the phenyl groups at the *meso* position of 5,10,15,20-tetraarylporphyrins were prepared in our laboratories and evaluated in vitro for their phototoxicity.[16,17] It was found that compounds bearing three mono-saccharide units are, in general, more phototoxic than symetrical compounds. Moreover, according to Bonnett[18] tetrahydroxyphenyl chlorins appears as more efficient in animal models than the corresponding porphyrin derivatives.

The objective of the present work was to explore how tri and tetra-*meta*-*O*-glucosylations of the chlorin macrocycle affect the photoactivity, cell internalization and subcellular localization in HT29 human adenocarcinoma cells. In vitro overall photobiological activity for the glucoconjugated chlorins has been compared to that for *m*-THPC.

Results

Synthesis and physical characteristic of glycoconjugated chlorins

m-THPC (**1**), its fully glucosylated derivative **4**, and the triglucosylated compounds **5** and **6** (Fig. 1) were prepared with a high yield from the corresponding porphyrins[19] by the diimide reduction procedure previously described.[20–22] The reduction process of triglucosylated porphyrin **3** gives the two possible isomeric chlorins **5**–**6**. The isomeric 2,3- and 7,8-*meta*-tri-glucosylated chlorins **5** and **6** were obtained as an inseparable mixture. These two compounds are different by the position of the reduced double bond in the macrocycle (Fig. 2). The required glucoconjugated chlorins **7**, and **8**/**9** were subsequently obtained in quantitative yield by treatment with MeONa/MeOH.[23] For all compounds, one principle peak (MH^+; no fragments), was observed in the positive ion mass spectra, corresponding to the intact chlorin macrocyle. Isotopic analysis indicated the presence of a protonated species $(M+1)^+$ with a very minor contribution of the unprotonated cation (M^+).

As observed for most meta-substituted tetra-arylporphyrins/chlorins, the *meta*-tetra-glucosylated derivative **4** existed as an equilibrium mixture of four atropoisomers at room temperature.[24] The ^{1}H NMR spectrum of this compound was poorly resolved between 20 and 55 °C. However, assignment of the resonances to individual atom types was achieved from 2-D homonuclear correlation spectroscopy (COSY) and heteronuclear multiple coherence (HMQC) experiments. The ^{1}H NMR spectrum of isomeric 2,3- and 7,8-*meta*-triglucosylated chlorins **5** and **6** showed two NH signals of equal intensity, at −1.48 and −1.58, indicating a 1/1 mixture. The corresponding ^{1}H NMR spectrum of the tri-glucoconjugated chlorin isomers **8** and **9** was similarly poorly resolved (mixture of two isomers and six atropoisomers), preventing interpretation. Small peaks at 8.88 ppm (H-pyrrole) and −2.90 ppm (HN) were observed in the ^{1}H NMR spectra for all chlorin products,

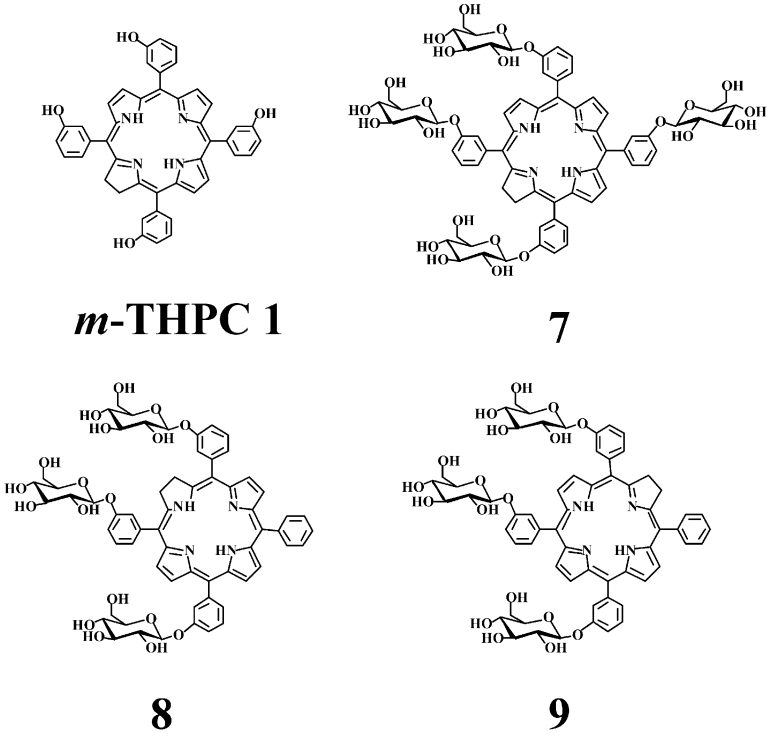

Figure 1. Chemical stucture of glucosylated derivatives.

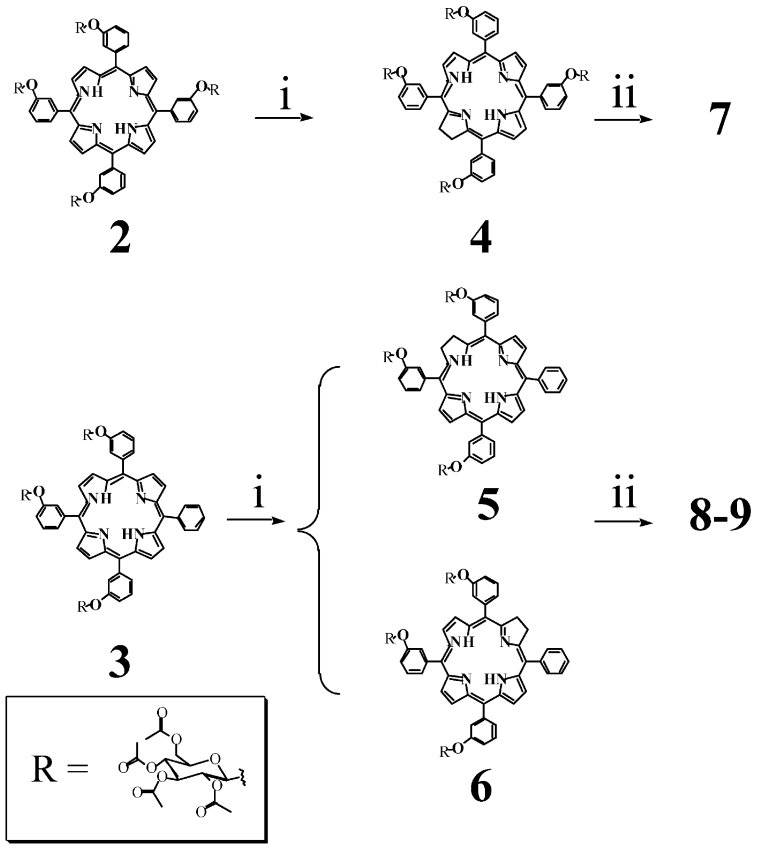

Figure 2. Synthesis of glucosylated derivatives: (i) (a) toluene-4-sulfonohydrazide, anhydrous K_2CO_3, dry pyridine, 100 °C, (b) *ortho*-chloranil, ethyl acetate, 20 °C; (ii) MeONa/MeOH, 20 °C.

indicating the presence of inseparable porphyrin side products (<10%). Similar features have been observed by Bonnett et al.[25] The octanol-water partition coefficients (LogPc) determined according to Kessel et al.[26] were found to be >3 for **1**, 1.45 for **8**/**9**, and −1.31 for **7**.

The absorption spectra of glucosylated chlorins **4**, **7**, **5**/**6** and **8**/**9** were typical of chlorin derivatives with a Soret band around 415 nm and a high extinction coefficient for the Q band maximum at 650 nm. It may be noted that the presence of glucosylated substituents results in an increase of extinction coefficients (Table 1) although electronic conjugation should not be significantly modified by the presence of sugar units. In aqueous medium, a large broadening of the Soret band together with an overall hypochromicity of the spectrum were observed, indicating the occurence of intermolecular association.[27,28]

Table 1. Molar extinction coefficients (ε), fluorescence emission maximum wavelength (λ_{max}) and fluorescence quantum yields (ϕ_F) of photosensitizers in solution in methanol

Photosensitizer	ε 416 nm (M^{-1} cm^{-1})	ε 514 nm (M^{-1} cm^{-1})	ε 650 nm (M^{-1} cm^{-1})	λ_{max} (nm)	ϕ_F
1	1.24×10^5	1.23×10^4	2.09×10^4	652	0.095
8/9	2.4×10^5	1.73×10^4	3.68×10^4	652	0.116
7	1.8×10^5	1.44×10^4	3.4×10^4	652	0.13

The original spectrum signature was partly restored by the addition of fetal calf serum (FCS) (10%) (data not shown). Fluorescence emission spectra were identical to that of *m*-THPC with a maximum at 652 nm and a weaker band around 720 nm. The fluorescence quantum yields were slightly enhanced by the glucosylation (Table 1). It may be noted that the value found for **1** is in good agreement with that determined by Bonnett et al.[29]

Phototoxicity

The phototoxicity of **1**, **7** and **8**/**9** was determined in human colorectal adenocarcinoma cells (HT29) cells by cell survival fraction measurements after incubation either in the dark or with exposure to 514 nm light with a fluence of 5, 10 and 25 J/cm^2 (Fig. 3). For **1** and **8**/**9**, toxicity in darkness was slight with a survival fraction around 98% over a concentration range of 1–8 μM. In contrast, **7** appeared to exhibit some dark cytotoxicity depending on the FCS concentration in the medium. Indeed, after incubation for 3 h in 2% FCS-containing medium, cell survival was only 51% at 4 μM, whereas it was essentially 100% in the presence of FCS10%. Figure 4 shows the concentration dependence of phototoxicity of the three sets of dyes **1**, **7**, **8**/**9** for a light fluence of 5 J/cm^2. For **8**/**9**, the survival fraction was minimum (2±0.6%) at a concentration as low as 2 μM, then remained constant up to 8 μM. In contrast, at 2 μM, the survival fraction was still 16±2% for **1** and 22±4% for **7**.

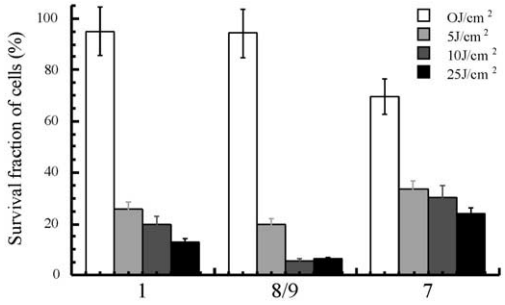

Figure 3. Survival fraction of HT 29 cells incubated (1 μM, 3 h) with **1** (*m*THPC), **8**/**9** [TPC(*m*-*O*-GluOH)$_3$] and **7** [TPC(*m*-*O*-GluOH)$_4$] in FCS containing medium (2%) and followed by exposure to 514 nm light. Each experiment (16 wells/experiments) was carried out in triplicate. Bars, standard error.

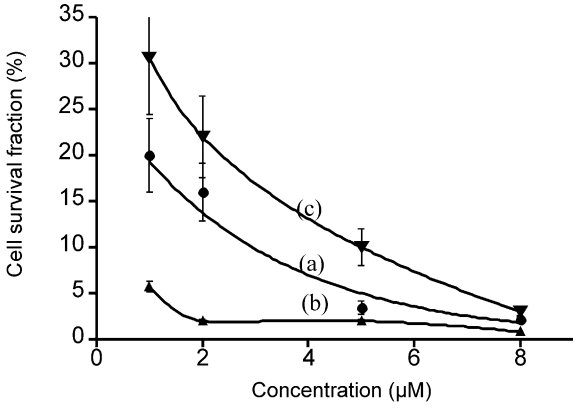

Figure 4. Concentration dependence of phototoxicity of (a) **1**, (b) **8**/**9** and (c) **7** in HT29. Cells were incubated for 3 h and exposed to 514 nm light with a light fluence of 5 J/cm^2. For each experiment, data have been averaged from intensity values determined on 30 individual cells. Experiments have been triplicated. Bars, standard error.

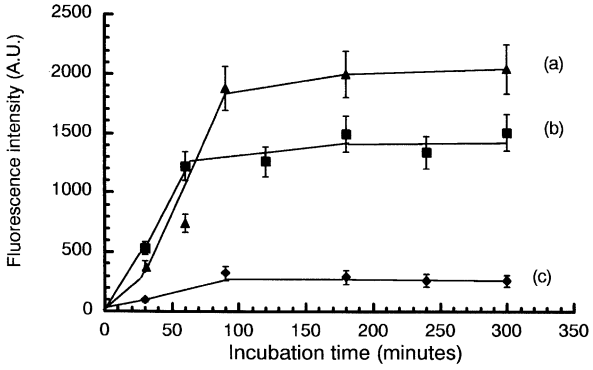

Figure 5. Cellular uptake time course as determined from the cellular fluorescence of HT29 cells incubated with (a) **1**, (b) **8**/**9** and (c) **7** (2 μM). Cellular fluorescence intensities were measured at 654 nm. For each experiment, data have been averaged from intensity values determined on 30 individual cells. Experiments have been triplicated. Bars, standard error.

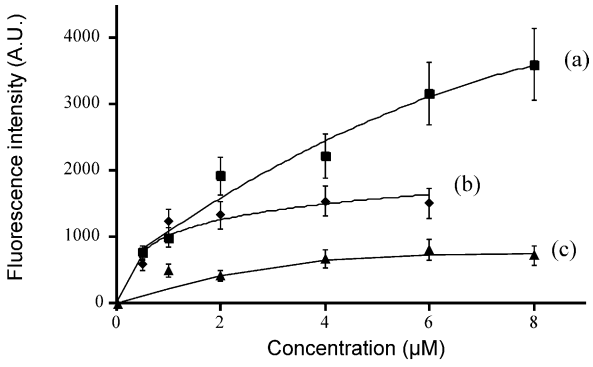

Figure 6. Concentration dependence of cellular uptake for (a) **1**, (b) **8**/**9** and (c) **7** in HT29 cells incubated for 3 h. For each experiment, data have been averaged from intensity values determined on 30 individual cells. Experiments have been triplicated. Bars, standard error.

Keeping in mind that the survival fraction in darkness was approximately 67 ± 7% at the same concentration, the photoactivity of **7** is effectively poor.

Cell internalization

Cellular uptake of reference compound **1** and glucoconjugated compounds **7**, and **8**/**9** was determined on the basis of the cellular fluorescence intensity. The cellular fluorescence spectrum of the cytoplasmic area of living single cells incubated with the chlorin derivatives was similar to that of the corresponding chlorin in solution, with a main peak slightly red shifted (654 nm) and a poorly resolved band around 720 nm. A contribution of cellular autofluorescence (maximum around 570 nm) only affected fluorescence intensity for short incubation times, and its contribution was deduced when necessary.

Figure 5 shows the time-course of **1**, **7** and **8**/**9** internalization. Drug uptake increased during the first 2 h, and reached a saturation value for incubation times higher than 2 h. It must be noted that similar levels of fluorescence intensities were found after 24 h incubation, indicating that drug release processes were negligible. Compared to **1**, the uptake of the compounds **8**/**9** and **7** was 30 and 80% less, respectively. It may be noted that cellular uptake can be correlated to the dye partition coefficient values, higher lipophilicity corresponding to greater uptake. The much lower uptake observed for the chlorin **7** bearing four glucose residues is consistent with the low phototoxicity observed. Most interesting, uptake and phototoxicity of **8**/**9** appear to not correlate. In fact, the intracellular concentration of **8**/**9** was found to be lower than for **1**, whereas its phototoactivity was higher.

Figure 6 illustrates the concentration uptake dependence for dyes **1**, **7** and **8**/**9**. A saturable process could be observed with glucoconjugated compounds **7** and **8**/**9** for concentrations higher than 2 μM. For *m*-THPC (**1**), saturation was not observed over the concentration range up to 8 μM.

The intracellular drug concentrations determined for cells incubated for 3 h at 6 μM were found to be 3.57×10^{-6}, 2.4×10^{-6} and 1.03×10^{-6} μmol/μg of proteins for **1**, **8**/**9** and **7**, respectively. It may be noted that concentrations followed the trend **1** > **8**/**9** > **7** which is consistent with the fluorescence measurements. The

ratio of intracellular concentrations of compounds **7** and **8**/**9** to **1** are comparable to the corresponding fluorescence intensity ratios (Fig. 6). Such a correlation between cellular extraction and fluorescence measurements shows that (in as far as fluorescence yields of the photosensitizers **1**, **7** and **8**/**9** in solution were quite similar) any eventual variations of fluorescence quantum yield resulting from the cellular environment or from some aggregate formation would be similar for the three compounds studied. Such a finding provides evidence that intracellular fluorescence variations reflect the internalized drug concentration.

Internalization of both **1** and **8**/**9** was strongly inhibited when incubations were carried out at 4 °C. Hence, cellular fluorescence could not be determined accurately. Extraction showed that **1** and **8**/**9** uptake was diminished, respectively, by 20 and 50% relative to the values at 37 °C. This result indicates a higher contribution of an active internalization process for **8**/**9** than for **1** in as far as it is generally accepted that active uptake process is substentially reduced by lowering the temperature of incubation. The temperature effect was not examined for **7** because of the weak internalization at 37 °C.

Preincubation of cells (15 min) with sodium azide (NaN_3), an inhibitor of the mitochondrial respiratory chain, was found to modify dyes take up to a different extent. A strong decrease of 60% in take up of **8**/**9** (3 h–6 μM) was observed for cells treated with NaN_3 (10 mM). In the same conditions the decrease was only 20% for **1**, and 60% inhibition of drug uptake was only achieved for cells treated with NaN_3 for a 100 mM concentration. These results suggest internalization of **8**/**9** is more energy consuming than for **1**.

Subcellular localization

The subcellular localization of **1**, **8**/**9** and **7** was examined by fluorescence imaging microscopy. For cells treated with **1**, the fluorescence was diffusively distributed throughout the cytoplasm, with some bright spots and a non fluorescent nuclear area (Fig. 7). In contrast, a punctate cytoplasmic fluorescence was observed with cells treated with **8**/**9**, the nucleus area remaining dark. When cells were co-incubated with the dye and Rhodamine 123 (a fluorescent probe specific of mitochondria) the observed fluorescence pattern (Fig. 8) suggested that **8**/**9** localized in the same subcellular region as Rhodamine 123. Long incubation time (24 h) did not significantly alter this intracellular fluorescence pattern. A similar distribution was observed with cells treated with **7**. Due to the low internalization of this compound, high concentrations were necessary to observe a fluorescence distribution. Mitochondria isolation experiments were carried out with cells treated with **1** and **8**/**9** (Experimental). The mitochondrial **8**/**9** fraction, as determined by absorption spectroscopy, represented 40–50% of the total intracellular dye concentration. In contrast, mitochondrial **1** fraction only represented 20–30% of the total concentration. These results clearly show that **8**/**9** exhibits a higher mitochondrial affinity than **1**.

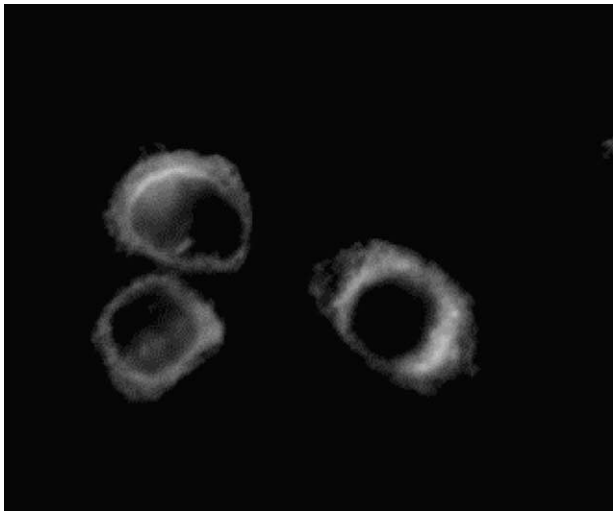

Figure 7. Fluorescence pattern of HT29 cells incubated with **1** (6 μM, 3 h incubation). Cells were illuminated using a filter set (BP 425 DF45; FT 450 DCLP; LP 600 ALP) .

Effect of serum on phototoxicity and cell uptake

Phototoxicity and drug internalization were not significantly different for incubations with or without FCS 2%. We have to keep in mind that incubation times were short enough not to damage cells by the absence of serum. For higher FCS concentrations (5%), cellular uptake as expressed by the ratio of cellular fluorescence measured in the presence of FCS (F) to that measured without FCS (F_0), was strongly decreased by the presence of FCS. The effect was similar for 8/9 ($F/F_0 = 41 \pm 6\%$) and 1 ($F/F_0 = 47 \pm 7\%$). In the presence of FCS 10%, 8/9 uptake was further diminished, and the F/F_0 ratio was only ($25 \pm 4\%$), whereas the ratio for 1 was unaffected (46%). The presence of FCS (10%) also affected phototoxicity (a 10-fold decrease for 8/9 and only a 3-fold decrease for 1). It may be noted that a similar decrease of 8/9 and 1 uptake was observed when incubations were performed in the presence of albumin at a concentration corresponding to FCS albumin content (see Experimental) indicating that non covalent binding with albumin could be mainly responsible for FCS effect observed.

Discussion

Glucosylation of the chlorin ring strongly modifies the photobiological activity of the reference molecule *m*-THPC (**1**). As seen, the symmetrical non amphiphilic tetraglucoconjugated chlorin **7** exhibits a poor photoactivity profile, and consequently does not present much interest for a potential clinical use. In contrast, the asymmetric compounds **8**/**9**, which are amphiphilic (see partition coefficient), display specific interesting biological properties.

As seen from the comparison of uptake and phototoxicity, serum effect is higher for **8**/**9** than **1** showing that intermolecular association with albumin would be more pronounced for **8**/**9** than for **1**. Photosensitizers

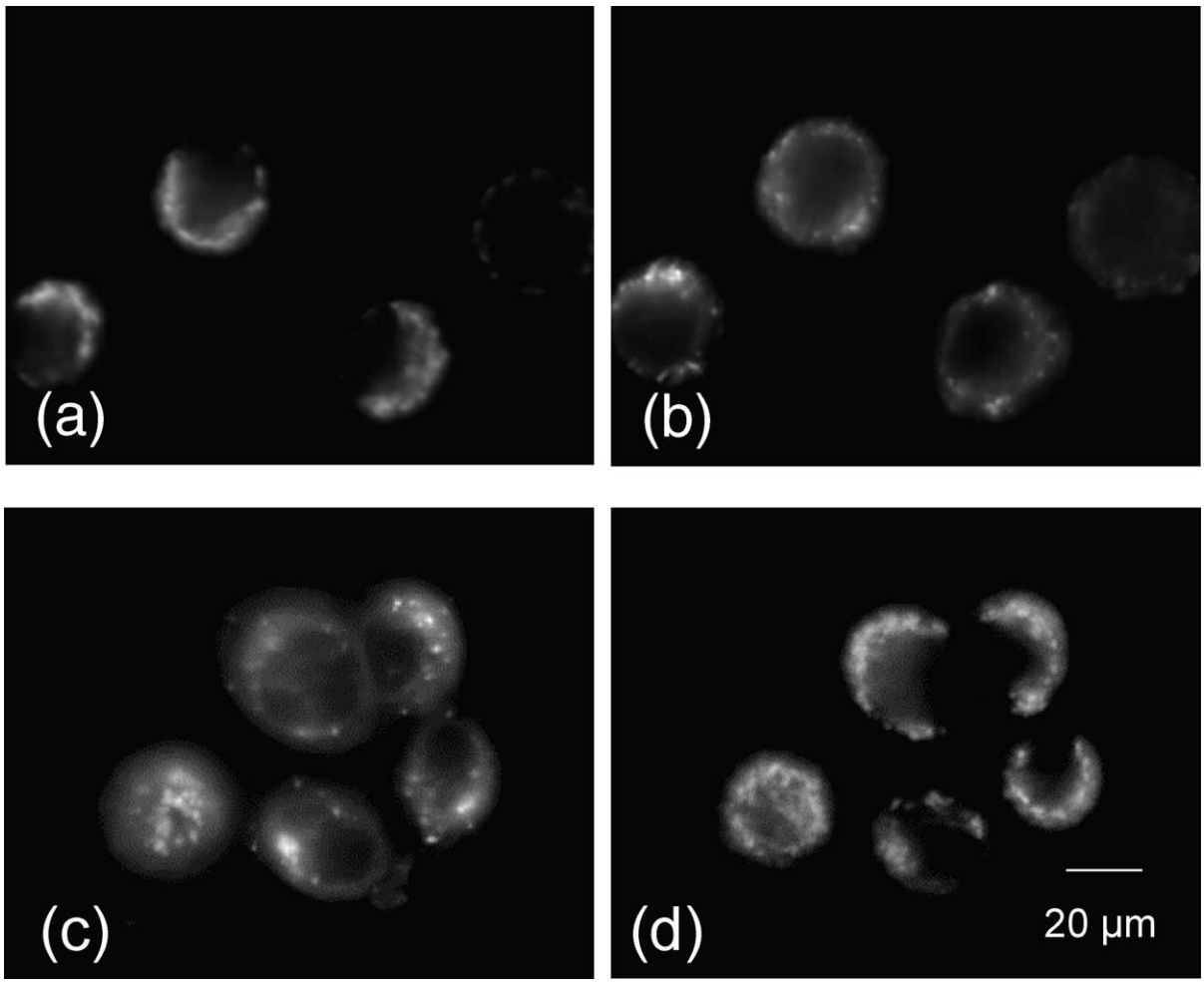

Figure 8. Fluorescence pattern of HT29 cells after co-incubated with **8**/**9** (**a**) (6 μM) and **7** (**c**) (8 μM) for 3 h and Rhodamine 123 (**b**,**d**) (5 μM) for 30 min. Cells were illuminated with a filter set using a filter set (BP 425 DF45; FT 450 DCLP; LP 600 ALP) for sensitizers and a FITC filter set for Rhodamine 123.

have been shown to bind to several proteins in plasma depending on their structure. The more hydrophobic sensitizers associate with lipoproteins,[30] while hydrophilic sensitizers associate more with albumin[31] and high molecular weight proteins. Albumin is by far, the most important drug carrier in blood. Plasma protein–drug interactions result in modifications in biological half-lives, transfer of drugs to tissues and distribution volume that are important parameters to consider for a potential in vivo use.

Cellular internalization of **8**/**9** and **1** appears to involve distinct processes. Compared to **1**, the **8**/**9** uptake is a saturable process (Fig. 6), inhibition of the cellular uptake at 4 °C is more pronounced and **8**/**9** uptake is more adenosine tri phosphate (ATP) energy dependent. These results suggest that **8**/**9** internalization occurs mainly via a carrier or receptor-mediated endocytosis. An active uptake process via LDL has been reported in literature for **1**.[32,33] However, our findings indicate that such a process would only be involved to a lesser extent and that passive diffusion has also to be considered.

The punctate fluorescence pattern observed by fluorescence microscopy suggests a mitochondrial location of **8**/**9**. The diffuse cytoplasmic fluorescence observed for cells treated with **1** is consistent with previous results reported in literature. According to Melnikova et al.[34] **1** is present in many organelles: endoplasmic reticulum, mitochondria and Golgi apparatus as well. Recently, Leung et al.[35] observed a similar diffuse cytoplasmic fluorescence pattern they ascribed to a lysosomal localization. The determination of mitochondrial concentration showed that both photosensitizers **1** and **8**/**9** are localized in mitochondria, but with a 2-fold enhancement of the mitochondrial affinity for the glucoconjugated compounds **8**/**9**. Localization in mitochondria is a general feature that is assumed to occur for most photosensitizers but to a different extent depending on the structure.[34] Amphiphilicity has been reported by several authors to be a parameter that favors a mitochondrial localization[12,36] which would be consistent with our findings. Subcellular localization is a determining parameter to consider in the photodynamic activity of a photosensitizer in as far as photodynamic processes take place in the site of formation because of a very short lifetime of oxygen reactive species[37] and mitochondria are usually considered as an efficient site for producing photodamages.

In summary, the asymmetrical triglucosylated chlorin **8**/**9** exhibits a high in vitro photoactivity and a preferential mitochondrial affinity. Mitochondrial localization may be important to the observation that, despite lower levels of cell uptake of **8**/**9** compared to **1**, the phototoxicity of the triglucosylated compound is superior. On the basis of these results obtained for **8**/**9** work is in progress to further evaluate the photodynamic activity of glycosylated chlorins in vivo.

Experimental

All reagents were purchased from Aldrich Chemical Co (Milwaukee, WI, USA). Toluen-4-sulfono hydrazide was purchased from Fluka. Merck silica gel 60 (0.040–0.060 mm) was used for column chromatography. Macherey-Nagel precoated plates (SIL G-200, 2 mm) were used for preparative thin layer chromatography. Dry pyridine was obtained by distillation on KOH and kept on 4 Å sieves. ^{1}H NMR spectra were obtained in the deuteriated solvents using a Brucker AM-300. Acidic impurities in chloroform-d_3 were removed with anhydrous K_2CO_3. Chemical shift values are given in ppm relative to tetramethyl silane (TMS). Mass spectrometry analysis was performed using a matrix-assisted laser desorption ionization-time of flight (MALDI-TOF) mass spectrometer (PerSeptive Biosystem Voyager Elite, Framingham, USA). UV–visible spectral characteristics and extinction coefficients were determined using a Varian DMS 200 spectrometer. A LS 50B spectrofluorimeter (Perkin–Elmer) equipped with a red sensitive R6872 photomultiplier was used for fluorescence measurements. Fluorescence quantum yields have been determined using Rhodamine B as a standard. Corrections have been made to take into account the respective spectral response of the detection system.

General procedure for the preparation of glucosylated chlorin derivatives

5, 10, 15, 20-Tetrakis[3-*O*-(2′, 3′, 4′, 6′-tetraacetyl-β-D-glucosyl)phenyl]-2, 3-chlorin, 4. TPP(*m*-*O*-GluOAc)$_4$ **2**[18] (350 mg, 0.175 mmol) and anhydrous K_2CO_3 (220 mg) were added to dry pyridine (8 mL) under argon. Toluene-4-sulfonohydrazide (65.6 mg, 0.35 mmol) was then added, and the mixture was heated under argon at 100–105 °C for 24 h. Further quantities of toluene-4-sulfonohydrazide (65.6 mg in 0.5 mL of dry pyridine) were added after 2, 4, 6 and 8 h. After cooling, the crude mixture was treated with ethyl acetate (55 mL), water (27.5 mL) and heated, at 100 °C, for 1 h. After cooling, the organic phase was separated and washed with HCl (2 M, 100 mL), water (75 mL) and saturated water solution of $NaHCO_3$. The presence of chlorin and bacteriochlorin was controlled by UV–visible spectroscopy (bands at 651 and 738 nm, respectively). *ortho*-Chloranil (110 mg) was slowly added to the stirred organic solution at 25 °C until the absorption peak at 735 nm (bacteriochlorin) disappeared. The solution was washed with aqueous solution of $NaHSO_3$ (5%, 100 mL), water (100 mL) and dried over anhydrous sodium sulfate. The filtered solution was concentrated under vacuum. The residue was purified by column chromatography on silica gel eluted by a mixture of methylene chloride/acetone (10/1, v/v). The pure product (red band) was crystallized from a mixture of methylene chloride/heptane (302 mg, yield 89%). Microanalysis calcd for $C_{100}H_{104}N_4O_{40}$, $2H_2O$: C, 58.94; H, 5.34; N, 2.76; Found C, 58.86; H, 5.40; N, 2.73. MALDI-TOF spectrum for $C_{100}H_{104}N_4O_{40}$: calcd 2000.62; Found M + 1: 2001.76. UV–visible spectrum in CH_2Cl_2 λ_{max} (ε L mmol^{-1} cm^{-1}): 417.5 (208); 516.5 (15.2); 543.5 (9.1); 597.5 (5.4); 651 (33.2). ^{1}H NMR ($CDCl_3$): 8.61 (d, 2H, pyrrole), 8.45 (d, broad, 2H, pyrrole), 8.22 (d, 2H, pyrrole, $J = 3$ Hz), 7.81 (broad, 4H, *para*-phenyl), 7.75 (broad, 4H, *ortho*-phenyl), 7.63 (broad, 4H, *ortho*-phenyl), 7.34 (broad, 4H, *meta*-phenyl), 5.34 (d, 4H, HC_1, 'ose', $J = 3.2$ Hz), 5.32 (m, 8H, HC_2, HC_3 'ose'), 5.17 (dd, 4H, HC_4 'ose'), 4.19 (m, 4H, HC_6 'ose'), 4.18 (m, 4H, HC_2, HC_3 pyrrole), 4.04 (m, 4H, HC_6 'ose'), 3.81 (m, 4H, HC_5 'ose'), 2.09 (s), 2.07 (s), 2.03 (s) (36H, $HC_{2,3,4}$ acetyl), 1.63–1.33 (s, 12H, HC_6 acetyl), −1.54 (s, 2H, NH). ^{13}C NMR ($CDCl_3$) 170.7 (C=O), 169.7 ($C_{1,4}$), 155.6 (*m*-phenyl), 152.5 ($C_{11,14}$), 143.3 (C_{meso} phenyl), 140.8 ($C_{6,19}$), 135.1 ($C_{6,9}$), 132.4 ($C_{12,13}$), 130.3 (phenyl), 129.7 (phenyl), 128.6 ($C_{7,8}$ or $C_{17,18}$), 127.7 (phenyl), 123.8 ($C_{7,8}$ or $C_{17,18}$), 123 ($C_{10,15}$), 122.4 (phenyl), 116.6 (phenyl), 112.3 ($C_{5,20}$), 99.4 (C_1 'ose'), 72.4 (C_5 'ose'), 71.9 ($C_{2/3}$ 'ose'), 71.1 ($C_{3/2}$ 'ose'), 68.7 (C_4 'ose'), 62.3 (C_6 'ose'), 36.1 (CH_2 chlorine), 20.9 ($C_{2,3,4}$ acetyl), 20.5 (C_6 acetyl).

5,10,15,20-Tetrakis(3-*O*-β-D-glucosylphenyl)-2,3-chlorin 7. Compound **4** (205 mg, 0.1 mmole) was dissolved in a mixture of dry methanol (20 mL) and dry methylene chloride (20 mL). 200 μL of sodium methanolate in methanol (1 M) was added to the solution, and the mixture was stirred 1 h 30 at room temperature. IWT® TMD-8 ion exchange resin (1 g) was then added and the mixture was stirred for 30 min. The reaction mixture was filtered and the recovered resin was washed with methanol. The titled product was obtained after evaporation under vacuum and crystallized from methanol, 1-2 dichloroethane solution (128 mg, yield 94%). Microanalysis calcd for $C_{68}H_{72}N_4O_{24}$, H_2O: C, 60.62; H, 5.54; N, 4.16; Found C, 60.32; H, 5.45; N, 4.20. UV–visible spectrum in MeOH λ_{max}, (ε L mmol^{-1} cm^{-1}): 415 (183.9); 515.5 (14.4); 542.5 (10.1); 596 (6.7); 650 (27.7). MALDI-TOF spectrum for $C_{68}H_{72}N_4O_{24}$ calcd 1328.45; Found M + 1: 1329.70. ^{1}H NMR (pyridine-d_5) 8.80, 8.75 (m, 2H, pyrrole), 8.37 (m, 2H, pyrrole), 8.27 (m, 2H, pyrrole), 8.11–7.64 (m, 8H, phenyl), 7.50–7.10 (m, 8H, phenyl), 6.65 (broad, 4H, OH), 5.97 (broad, 4H, HC_1 'ose'), 4.42 (m, 22H, $HC_{2/3/4}$ 'ose'), 4.55 (m, 4H, HC_{6a} 'ose'), 4.36 (m, 4H, HC_{6a} 'ose'), 4.13 (m, 8H, HC_5 'ose' and $HC_{2,3}$ chlorine), −1.33 (s, 2H, NH).

^{13}C NMR (pyridine-d_5) 158.4, 157.3 (*m*-*O*-phenyl), 144.7, 144 (C_{meso1} phenyl), 129.7, 129.3 (*p*-phenyl), 128.6 (*m*-phenyl), 128.3 (*m*-phenyl or $CH_{7,8}$ or $CH_{17,18}$), 124 ($CH_{12,13}$ and $CH_{7,8}$ or $CH_{17,18}$), 121.5, 121, 120.4, 116.4, 116.2 (*o*-phenyl), 102.4 (C_1 sugar), 79 (C_5 sugar), 78.5, 75.2, 71.2 ($C_{2/3/4}$ sugar), 62.3 (C_6 sugar), 35.9, 35.3 (CH_2 chlorine).

5,10,15-Tri[3-*O*-(2′, 3′, 4′, 6′-tetraacetyl-β-D-glucosyl)-phenyl]-2, 3-chlorin and 5, 10, 15-tri[3-*O*-(2′, 3′, 4′, 6′-tetraacetyl-β-D-glucosyl) phenyl]-7, 8-chlorin, isomers 5–6. Compounds **5–6** (in inseparable mixture; 50/50) were prepared from TPP(*m*-O-GluOAc)$_3$ **3**[18] by the method described for the synthesis of **4**. Yield of isomers 72%. Microanalysis calcd for $C_{86}H_{86}N_4O_{30}$, $2H_2O$: C, 61.06; H, 5.36; N, 3.31; Found C, 61.01; H, 5.15; N, 3.29. UV–vis spectrum in CH_2Cl_2: λ_{max}, nm (ε L mmol^{-1} cm^{-1}) : 417.5 (272.9); 516.5 (19.2); 544 (13.3); 596.5 (9.1); 650.5 (35). ^{1}H NMR ($CDCl_3$) 8.59 (m, 2H, pyrrole), 8.42 (m, 2H, pyrrole), 8.22 (m, 2H, pyrrole), 8.08 (m, 1H, phenyl), 8.0–7.50 (m, 12H, phenyl), 7.50–7.29 (m, 4H, phenyl), 5.33 (m, 9H, HC_1, HC_2, HC_3 'ose'), 5.15 (m, 3H, HC_4 'ose'), 4.17 (m, 6H, HC_6 'ose'), 4.06 (broad d, 2H, HC_2 or HC_3 and HC_7 or HC_8, pyrrole, $J = 12.8$ Hz), 3.98 (broad d, 2H, HC_3 or HC_2 and HC_8 or HC_7, pyrrole,$J = 12.1$ Hz), 2.08 (s), 2.06 (m), 2.02 (s), 1.99 (m), 1.98 (s) (36H, acetyl), −1.48 (s), −1.58 (s) (2H, NH).

^{13}C NMR ($CDCl_3$) 170.4 (C=O), 152 ($C_{11,\ 14}$), 151 (*m*-phenoxy), 143 (C_{meso} phenyl), 141 ($C_{6,\ 19}$ chlorine), 135 ($C_{9,\ 16}$ chlorine), 133.6 (*p*-phenyl), 131.8 ($C_{12,13}$ chlorine), 127.8 ($C_{7,8/17,18}$ chlorine), 123.2 ($C_{7,8/17,18}$ chlorine), 99.6 (C_1 'ose'), 73.7 ($C_{2/3/4}$ 'ose'), 72.5 (C_5 'ose'), 71.7 ($C_{2/3/4}$ 'ose'), 68.7 ($C_{2/3/4}$ 'ose'), 62.2 (C_6 'ose'), 20.3 (CH_3).

5,10,15-Tri(3-*O*-β-D-glucosylphenyl)-2, 3-chlorin and 5,10,15-tri(3-*O*-β-D-glucosylphenyl)-7, 8-chlorin, isomers 8/9. These products were prepared by the method described for the synthesis of **7**. Yield of isomers 80%. Microanalysis calcd for $C_{62}H_{62}N_4O_{18}$ H_2O: C, 63.69; H, 5.52; N, 4.79; Found C, 63.29; H, 5.38; N 4.90. UV–vis spectrum in MeOH: λ_{max}, nm (ε L mmol^{-1} cm^{-1}) : 414.5 (237.9), 515 (17.3), 542 (12), 595.5 (8), 649.5 (32.8). MALDI TOF spectrum for $C_{62}H_{62}N_4O_{18}$: calcd 1150.40; Found M + 1: 1151.52. Partial ^{1}H NMR (pyridine-d_5) 8.78–8.73 (m, 2H, pyrrole), 8.36–8.26 (m, 4H, pyrrole), 8.10–7.62 (m, 17H, phenyl), 5.96 (d, 3H, HC_1 'ose'), 4.52 (m, 3H, HC_6 'ose'), 4.42 (m, 9H, $HC_{2,\ 3,\ 4}$ 'ose'), 4.12 (m, 3H, HC_6 'ose'), −1.28 (s, 2H, NH). Partial ^{13}C NMR (pyridine-d_5) 158 (*m*-phenoxy), 144 (*meso*-phenyl), 135–134.5 ($C_{7,8/17,18}$ chlorine), 132.8–128.5 ($C_{12,13}$ chlorine), 123.9–123.4 ($C_{7,8/17,18}$ chlorine), 102.4 (C_1 'ose'), 79 (C_5 'ose'), 78.7 ($C_{2/3/4}$ 'ose'), 75.2 ($C_{2/3/4}$ 'ose'), 71.4 ($C_{2/3/4}$ 'ose'), 62.4 (C_6 'ose'), 36 (CH_2 chlorine).

General procedure for in vitro experiments

Cell culture conditions. Human colorectal adenocarcinoma cells (HT29) were allowed to grow to confluence in Dulbecco's modified Eagle's medium (DMEM) without phenol red and supplemented with 10% FCS, glutamine and antibiotics. All reagents were from Bio-Media (France). Cells were subcultured by dispersal with 0.25% trypsin and seeded (10^6 cells/mL). For incubations, stock solutions (5 mg/mL) were prepared in dimethyl sulfoxide (DMSO) and dilutions were performed in culture medium in the presence of 2% FCS unless otherwise specified. FCS was from Bio Media (France), with a total protein concentration of 37.5 g/L and albumin content of 26.1 g/L. For experiments performed at 4 °C, cells were incubated for 2 h with cold solution kept at 4 °C and then washed with cold phosphate buffer saline (PBS). For microspectrofluorimetric and fluorescence imaging experiments, cells were grown in plastic Petri dishes and were washed after incubation and prior to measurements.

Photocytotoxicity assay. Cells were seeded into 96-well plates at 10^5 cells/mL (0.2 mL per well) and allowed to grow for 24 h in an incubator (5% CO_2, 37 °C, humidified atmosphere) (Jouan, France). On the day of experiment, the culture medium was removed and 200 μL of fresh DMEM with 2% FCS containing photosensitizers at a final concentration between 1 and 8 μM were added in each well. Cells were incubated and then washed before fresh complete medium was added. Irradiations were performed at 514 nm with an Ar^+ laser (Spectra Physics-2020) in sterile conditions. Cells were incubated and then washed twice with PBS before fresh complete medium was added. Irradiations were performed at 514 nm with an Ar^+ laser (Spectra Physics-2020) in sterile conditions. The light was transmitted by a silica optical fiber (core diameter 200 μm, N.A. 0.22) equipped with a diffuser (Medlight, Switzerland) in order to obtain a uniform light delivery to the whole plate (130 mm spot diameter). The power was calibrated with an energy meter (Spectra Physics-407), and irradiation times were adjusted in order to obtain fluences of 5, 10 and 25 J/cm^2. Controls were as follows: wells containing cells treated with photosensitizer but not exposed to light, wells containing cells without photosensitizer and without light, wells containing cells without photosensitizer and exposed to light.

Cell viability was measured 24 h later by determination of mitochondrial activity using the 3-(4,5-dimethylthiazol-2-yl) diphenyltetrazolium bromide (MTT) assay according to the method described by Mosmann.[38] At the time of counting, 100 μL of a DMEM-MTT (0.5 mg/mL) solution were added to each well and replaced by 200 μL of DMSO 4 h later. Optical densities of microplates were determined at 570 and 640 nm using a Labsystem®. Each experiment (16 wells/experiment) was carried out in triplicate.

Cellular internalization. Microspectrofluorimetry. Fluorescence intensity measurements from a cytoplasmic area of single living cells after sensitizer incubation were performed using a laser confocal microspectrofluorimeter which has been developed in our laboratory.[39] Excitation was performed with the 514 nm line of an Ar^+ laser and a long-pass filter (MTOJ560) was used on the emission path. Excitation beam was focused on a cell area of 1 μm^2 with a ×63 Zeiss plan Neofluar objective (NA 1.25), directly immersed in RPMI solution. The analyzed cellular volume was about 10 μm,[3] which was smaller than the cell volume, but large enough to take into account the heterogeneity of the cellular drug distribution. Fluorescence spectra were recorded in the 550–830 nm spectral region with an accumulation time of 0.5–1 s. For each experiment, measurements were carried out on 30 individual cells. It

must be noted that in these experimental conditions the cellular emission only results from the internalized fluorophores and can thus considered to reflect their concentration. For experiments carried out at 4 °C cells were incubated for 2 h, washed with cold PBS and left to 20 °C before fluorescence measurements.

Cellular extraction. Treated cells were washed three times with cold PBS and then removed using a cell scraper. Three milliliters of ethyl acetate were added to cell suspension in PBS after sonication. The resulting solution was left 30 min with constant shaking and then centrifuged at 1600*g* for 10 min. Supernatant was removed and dye concentration was determined by spectrophotometry. Protein concentration was determined using Lowry's method (Peterson et al.)[40] using a protein assay (Kit P56 56, Sigma Aldrich, France).

Determination of intracellular localization. Fluorescence microscopy. Experiments were carried out with a Nikon epifluorescence microscope (Optiphot-2) equipped with a Nipkow wheel coaxial-confocal attachment (Technical Instruments, model K2SBIO). Treated cells were in Petri dishes and viewed with a ×63 immersed objective in DMEM. A cooled CCD camera (RTEA 1317 K1CCD, Princeton Instrument) detected fluorescence images. Specific organelles staining probes (Molecular Probe Inc.) were used. Mitochondria were stained with Rhodamine 123. Cells were incubated for 1 min. A filter set (BP 425 DF45; FT 450 DCLP; LP 600 ALP) was used for sensitizers and a FITC filter set (BP450-FT510, LP 520) was used with Rhodamine.

Isolation of cell mitochondria. Mitochondria were isolated by differential centrifugation according to Pedersen et al.[41] All operations were carried out at 4 °C. Cells were removed using a cell scraper and suspended in 0.25 M ice-cold sucrose. Cell membranes were disrupted using a Dounce device. Suspension was centrifuged for 8 min at 630*g*; the supernatant was then removed and centrifuged for 15 min at 6800*g*. Sucrose was added to the pellet which was centrifuged twice for 15 min at 9800*g*. The last pellet represents the mitochondrial fraction. Dye concentration were measured by spectrophotometry.

Acknowledgements

This work was supported by the 'Association de la recherche contre le cancer' grant No. 5334. The authors wished to thank Dr. J. C. Blais for MALDI TOF analysis.

References and Notes

1. Hsi, R. A.; Rosenthal, D. I.; Glatstein, E. *Drugs* **1999**, *57*, 725.
2. Bonnett, R. *Chem. Soc. Rev.* **1995**, *24*, 19.
3. Savary, J. F.; Monnier, Ph.; Fontolliet, C.; Mizeret, J.; Wagnieres, G.; Braichotte, D.; van den Bergh, H. *Arch. Otolaryngol. Head Neck Surg.* **1997**, *123*, 162.
4. Radu, A.; Wagnieres, G.; van den Bergh, H.; Monnier, Ph. *Gastrointest. Endosc. Clin. N. Am.* **2000**, *10*, 439.
5. Niamen Konan, Y.; Gurny, R.; Alléman, E. *J. Photochem. Photobiol. B: Biol.* **2002**, *66*, 89.
6. Alléman, E.; Brasseur, N.; Benrezzak, D.; Rousseau, J.; Kudrevich, S. V.; Boyle, R. W.; Leroux, J. C.; Gurny, R.; van Lier, J. E. *J. Pharm. Pharmacol.* **1995**, *47*, 382.
7. Alléman, E.; Rousseau, J.; Brasseur, N.; Kudrevich, S. V.; Lewis, K.; van Lier, J. E. *Int. J. Cancer* **1996**, *66*, 821.
8. Lenaerts, V.; Labib, A.; Chouinard, F.; Rousseau, J.; Ali, H.; van Lier, J. E. *Eur. J. Biopharm.* **1995**, *41*, 38.
9. MacDonald, I. J.; Dougherty, T. *J. Porphyrins and Phthalocyanines* **2001**, *5*, 105.
10. Margaron, Ph.; Grégoire, M.-J.; Scasnar, V.; Ali, H.; van Lier, J. E. *Photochem. Photobiol.* **1996**, *63*, 217.
11. Boyle, R. W.; Dolphin, D. *Photochem. Photobiol.* **1996**, *64*, 469.
12. Moser, J. G.; Montforts, F. P.; Kusch, D.; Vervoorts, A.; Kirsch, D.; Berghahn, M.; Akgün, N.; Rueck, A.; Andrees, S.; Wagner, B. *Proc. SPIE. Int. Soc. Opt. Eng.* **1996**, *2924*, 22.
13. Sol, V.; Blais, J.-C.; Carré, V.; Granet, R.; Guilloton, M.; Spiro, M.; Krausz, P. *J. Org. Chem.* **1999**, *64*, 4431.
14. Sylvain, I.; Zerrouki, R.; Granet, R.; Huang, Y. M.; Lagorce, J.-F.; Guilloton, M.; Blais, J.-C.; Krausz, P. *Bioorg. Med. Chem.* **2002**, *10*, 57.
15. Zheng, G.; Graham, A.; Shibata, M.; Missert, J.; Oseroff, A. R.; Dougherty, T. J.; Pandey, R. K. *J. Org. Chem.* **2001**, *66*, 8709.
16. Momenteau, M.; Oulmi, D.; Maillard, Ph.; Croisy, A. *SPIE Photodynamic Ther. Cancer II* **1994**, *2325*, 13.
17. Momenteau, M.; Maillard, Ph.; de Belinay, M. A.; Carrez, D.; Croisy, A. *J. Biomed. Optics* **1999**, *4*, 1.
18. Bonnett, R. In *Chemical Aspects of Photodynamic Therapy*; Advanced Chemistry Texts; Gordon and Breach Science, The Netherlands: 2000; p 167, 190.
19. Oulmi, D.; Maillard, Ph.; Guerquin-Kern, J.-L.; Huel, C.; Momenteau, M. *J. Org. Chem.* **1995**, *60*, 1554.
20. Whitlock, H. W.; Hanauer, R.; Oster, M. Y.; Bower, B. K. *J. Amer. Chem. Soc.* **1969**, *91*, 7485.
21. Bonnett, R.; Nizhnik, A. N.; White, S. G.; Berembaum, M. C. *J. Photochem. Photobiol. B: Biol.* **1990**, *6*, 29.
22. Mikata, Y.; Onchi, Y.; Shibata, M.; Kakuchi, T.; Ono, H.; Ogura, S.-I.; Okura, I.; Yano, S. *Biorg. Med. Chem. Lett.* **1998**, *8*, 3543.
23. Zemplén, G. *Ber. Dtsch. Chem. Ges.* **1927**, 1555.
24. Gottwald, L. K.; Ullman, E. F. *Tetrahedron Lett.* **1969**, *36*, 3071.
25. Bonnett, R. Private communication.
26. Kessel, D. *Biochem.* **1977**, *16*, 3443.
27. Oulmi, D.; Maillard, Ph.; Vever-Bizet, C.; Momenteau, M.; Brault, D. *Photochem. Photobiol.* **1998**, *67*, 511.
28. Csik, G.; Balog, E.; Voszka, I.; Tölgyesi, F.; Oulmi, D.; Maillard, Ph.; Momenteau, M. *J. Photochem. Photobiol. B: Biol.* **1998**, *44*, 216.
29. Bonnett, R.; Charlesworth, P.; Djelal, B. D.; Foley, S.; Mc Garvey, D. J.; Truscott, T. G. *J. Chem. Soc., Perkin Trans. 2* **1999**, 325.
30. Maziere, J. C.; Morliere, P.; Santus, R. *J. Photochem. Photobiol. B* **1991**, *8*, 351.
31. Mori, M.; Kuroda, T.; Obana, A.; Sakata, I.; Hirano, T.; Nakajima, S.; Hikida, M.; Kumagai, T. *Jpn. J. Cancer Res.* **2000**, *91*, 845.
32. Kessel, D. *Int. J. Clin. Pract.* **1999**, *53*, 263.
33. Michael-Titus, A. T.; Whelpon, R.; Yaqub, Z. *Br. J. Clin. Pharmacol.* **1995**, *40*, 594.
34. Melnikova, V. O.; Bezdetnaya, L. N.; Bour, C.; Festor, E.; Gramain, M. P.; Merlin, J. L.; Potapenko, A. Y.; Guillemin, F. *J. Photochem. Photobiol. B: Biol.* **1999**, *49*, 96.

35. Leung, W. N.; Sun, X.; Mak, N. K.; Yow, C. M. *Photochem. Photobiol.* **2002**, *75*, 406.
36. Oleinick, N. L.; Evans, H. H. *Radiation Res.* **1998**, *150* (Suppl.), S146.
37. Moan, J.; Berg, K. *Photochem. Photobiol.* **1991**, *53*, 549.
38. Mosmann, T. *J. Immunol. Meth.* **1983**, *65*, 55.
39. Blais, J.; Amirand, C.; Ballini, J. P.; Debey, P.; Foultier, M. T.; Patrice, T. *J. Photochem. Photobiol. B: Biol.* **1995**, *27*, 225.
40. Peterson, G. L. *Anal. Biochem.* **1977**, *83*, 346.
41. Pedersen, P. L.; Greenawalt, J. W.; Reynafarje, B.; Hullihen, J.; Decker, G. L.; Soper, J. W.; Bustamente, E. *Methods Cell. Biol.* **1978**, *20*, 411.